Ex Situ Atomic Force Microscopy Analysis of β-Amyloid Self-Assembly and Deposition on a Synthetic Template

Chanki Ha† and Chan Beum Park*,†,‡,§

Science and Engineering of Materials (SEM) Interdisciplinary Program and Department of Chemical and Materials Engineering, Arizona State University, Tempe, Arizona 85287

Received January 16, 2006. In Final Form: May 1, 2006

The β-amyloid (Aβ) deposition, which is the conversion of soluble Aβ peptides to insoluble plaques on a surface, is an essential pathological process in Alzheimer's disease (AD). The identification and characterization of possible environmental factors that may influence amyloid deposition in vivo are important to unveil the underlying etiology of AD. According to the amyloid cascade hypothesis, diffuse plaques are initial and visual deposits in the early event of AD, leading to amyloid plaques. To study amyloid deposition and growth in vitro, we prepared a synthetic template by immobilizing Aβ seeds on an *N*-hydroxysuccinimide ester-activated solid surface. According to our analysis with an ex situ atomic force microscope, the formation of amyloid plaque-like aggregates was mediated by the interaction between Aβ in a solution and on a synthetic template, suggesting that Aβ oligomers function well as seeds for amyloid deposition. It was observed that insoluble amyloid aggregates formed on the template surface serve as a sink of soluble Aβ in a solution as well as mediate the formation of intermediates in the pathway of amyloid fibrillization in a solution. Relative seeding efficiencies of fresh monomers, oligomers, and fully grown fibrils were analyzed by measuring the deposited plaque volume and its height distribution through atomic force microscopy. The result revealed that oligomeric forms of Aβ act more efficiently as seeds than monomers or fibrils do. Fluorescence spectroscopy with thioflavin T confirmed that amyloid aggregate formation proceeds in a concentration-dependent manner. Analysis with Fourier transform infrared spectroscopy indicated a progressive transition of soluble Aβ42 monomer to amyloid fibrils having antiparallel β-sheet structure on the template. Furthermore, studies on the interaction between Aβ40 and 42, two major variants of Aβ derived from the amyloid precursor protein, showed that amyloid aggregate formation on the surface was accelerated further by the homogeneous association of soluble Aβ42 onto Aβ42 seeds than by other combinations. A slightly acidic condition was found to be unfavorable for amyloid formation. This study gives insight into understanding the effects of environmental factors on amyloid formation via the use of a synthetic template system.

Introduction

The presence of extracellular amyloid deposits in the core of neuritic plaques in the brain is one of the key neuropathological features of Alzheimer's disease (AD).[1−3] Within and near these amyloid deposits, an extensive inflammatory response had been reported to occur, along with activated microglia and reactive astrocytes.[4,5] The major constituents of amyloid plaques are β-amyloid (Aβ) 40 and 42 peptides,[3,6,7] which are normally derived as soluble proteolytic products of the amyloid precursor protein (APP), a large integral membrane protein in the brain.[3,8] Although both Aβ peptides are usually colocalized in the plaques, Aβ42 is more amyloidogenic and pathogenic due to its hydrophobic property.[9,10]

According to the amyloid cascade hypothesis of AD,[3] the initial deposition of aggregated Aβ42 as diffuse plaques is critical for further growth of the amyloid plaque. Aβ42 oligomers or protofibrils had been known to work as diffuse plaques in the early stages of AD.[1,11,12] For a better understanding of AD, it is important to elucidate the time evolution of the diffuse plaques by means of the deposition of soluble amyloid precursor peptides. The examination of environmental factors accelerating amyloid plaque formation and growth is an important key to unveiling the underlying etiology of AD.

To date, however, the requirement for brain tissue plaque and its centrifugation has made the amyloid deposition study extremely difficult and cumbersome. The current method for studying amyloid deposition is often time-consuming, expensive, and labor-intensive and may take anywhere from several months to several years, making the analytical process very slow. Therefore, there is a critical need for an in vitro model system that can enable an investigation of the temporal evolution of amyloid plaque growth under different environmental conditions.

In our present work, we have prepared a synthetic template by immobilizing Aβ seeds onto an *N*-hydroxysuccinimide ester (NHS)-activated solid surface in an effort to imitate amyloid

* To whom correspondence should be addressed. Phone: (480) 965-0362. Fax: (480) 965-0037. E-mail: cbpark@asu.edu.

† SEM Interdisciplinary Program.

‡ Department of Chemical and Materials Engineering.

§ Current address: Department of Materials Science and Engineering, Korea Advanced Institute of Science and Technology, 373-1 Guseong-dong, Yuseong-gu, Daejeon, 305-701 Republic of Korea. Tel: +82-42-869-3340. Fax: +82-42-869-3310. E-mail: parkcb@kaist.ac.kr.

(1) Selkoe, D. J.; Schenk, D. *Annu. Rev. Pharmacol. Toxicol.* **2003**, *43*, 545−584.

(2) Lahiri, D. K.; Farlow, M. R.; Greig, N. H.; Sambamurti, K. *Drug Dev. Res.* **2002**, *56*, 267−281.

(3) Selkoe, D. J. *Physiol. Rev.* **2001**, *81*, 741−766.

(4) Matsuoka, Y.; Picciano, M.; Malester, B.; LaFrancois, J.; Zehr, C.; Daeschner, J. M.; Olschowka, J. A.; Fonseca, M. I.; O'Banion, M. K.; Tenner, A. J.; Lemere, C. A.; Duff, K. *Am. J. Pathol.* **2001**, *158*, 1345−1354.

(5) Stalder, M.; Phinney, A.; Probst, A.; Sommer, B.; Staufenbiel, M.; Jucker, M. *Am. J. Pathol.* **1999**, *154*, 1673−1684.

(6) Mori, H.; Takio, K.; Ogawara, M.; Selloe, D. J. *J. Biol. Chem.* **1992**, *267*, 17082−17086.

(7) Masters, C. L.; Simms, G.; Weinman, N. A.; Multhaup, G.; McDonald, B. L.; Beyreuther, K. *Proc. Natl. Acad. Sci. U.S.A.* **1985**, *82*, 4245−4249.

(8) Goldgaber, D.; Lerman, M. I.; McBride, O. W.; Saffiotti, U.; Gajdusek, D. C. *Science* **1987**, *235*, 877−880.

(9) Bitan, G.; Kirkitadze, M. D.; Lomakin, A.; Vollers, S. S.; Benedek, G. B.; Teplow, D. B. *Proc. Natl. Acad. Sci. U.S.A.* **2003**, *100*, 330−335.

(10) Jarrett, J. T.; Berger, E. P.; Lansbury, P. T. *Biochemistry* **1993**, *32*, 4693−4697.

(11) Lemere, C. A.; Blusztajn, J. K.; Yamaguchi, H.; Wisniewski, T.; Saido, T. C.; Selkoe, D. J. *Neurobiol. Dis.* **1996**, *3*, 16−32.

(12) Tagliavini, F.; Giaccone, G.; Frangione, B.; Bugiani, O. *Neurosci. Lett.* **1988**, *93*, 191−196.

10.1021/la0601511 CCC: $33.50
Published on Web 07/06/2006

plaque growth in vitro. Previously we successfully simulated insulin amyloid formation on a solid surface through the use of a similar synthetic template.[13] It was found that a synthetic template with partially unfolded insulin on its surface can induce the conformational change of native insulin in a solution, leading to the growth of insulin amyloid fibrils on the surface. On the basis of our previous results, we are investigating the deposition of soluble Aβ molecules onto a surface of the synthetic template and the formation of amyloid plaque-like aggregates. Progressive Aβ deposition was visualized and quantified by the use of ex situ atomic force microscopy (AFM). AFM images showed that the immobilized Aβ template strongly induced amyloid formation. Furthermore, amyloid deposits were able to accelerate Aβ deposition and simultaneously induce the formation of Aβ oligomers and protofibrils in a solution phase. The plaque-like growth on the synthetic template was further confirmed by thioflavin T (ThT)-induced fluorescence and Fourier transform infrared spectroscopy (FT-IR). In addition, in the current work we investigate the effects of the following factors on amyloid growth rate and morphology: (1) seeding abilities of fresh, oligomeric, and fibrillar Aβ42; (2) interaction between Aβ40 and Aβ42; (3) solution pH. According to our study, environmental factors influence the Aβ deposition process significantly and may play an important role in amyloid plaque formation.

Experimental Section

Materials. Aβ40 and Aβ42 were obtained from rPepetide Co. (Athens, GA). Bovine serum albumin (BSA), (3-aminopropyl)-triethoxysilane (APTS), *N*,*N*′-disuccinimidyl carbonate (DSC), *N*,*N*-dimethylformamide (DMF), 1,1,1,3,3,3-hexafluoro-2-propanol (HFIP), and ThT were purchased from Sigma-Aldrich (St. Louis, MO). Micro cover glasses were obtained from VWR Scientific (West Chester, PA).

Preparation of Peptides. Lyophilized peptides were dissolved to 2.5 mg/mL in 100% HFIP and sonicated in a water bath for 3 min to solubilize any existing aggregates. The peptide solution was separated into aliquots in sterile microcentrifuge tubes. The HFIP solvents were evaporated in a vacuum using Corning Pyrex brand vacuum desiccators (Fisher Scientific International Inc.), and the remaining peptide film was stored at −20 °C. Prior to use, the peptide was resuspended in dimethyl sulfoxide (Me_2SO) and diluted with phosphate-buffered saline (PBS), pH 7.4, to a concentration of 30 μM. After being immediately vortexed for 30 s, the Aβ solutions containing 5% Me_2SO were incubated at 37 °C.

Preparation of Synthetic Templates for the Immobilization of Aβ Seeds. We prepared an NHS-activated solid surface as follows for a covalent attachment of Aβ seeds to the surface. First, glass slides were cleaned for 12 h with a piranha solution of 70% H_2SO_4/30% H_2O_2 (7:3, v/v), rinsed with deionized water, and dried by N_2. The slides were subsequently aminopropylated with a 3% solution of APTS in ethanol/water (95:5, v/v) for 1 h. The aminopropylated surfaces were dipped in 100% ethanol and cured at 110 °C for 1 h. After being cooled and washed with 95% ethanol, the slides were activated with NHS. This solution was prepared as a 20 mM DSC solution in a sodium bicarbonate buffer (50 mM, pH 8.5). The slides were incubated for 3 h at room temperature, followed by washing with deionized water and drying with N_2.

Amyloid Deposition and Growth on a Synthetic Template. The synthetic template was prepared by uniformly placing a 7 μL (AFM and FT-IR samples) or 30 μL (ThT fluorescence samples) aliquot of Aβ solution onto the entire surface of an NHS-activated glass slide for a few minutes. The remaining solution on the glass was blown off by N_2. Sites with remaining functionalities were blocked by exposing the template to a solution of 0.1% BSA in a 50 mM phosphate buffer (pH 7.5). The template was extensively washed with a 50 mM phosphate buffer (pH 7.5) for 1 h, washed with deionized water for 45 min, and dried with N_2. Only stable Aβ aggregates against dissolution in aqueous buffers remained. Unless indicated specifically, the synthetic template was made by following the procedures mentioned above. Amyloid growth on the template was made by incubating a synthetic template in fresh Aβ in PBS (pH 7.4) containing 5% Me_2SO at 37 °C. After incubation, the substrate was washed with deionized water and dried with N_2 for further analysis.

Ex Situ AFM. Visualization of amyloid growth on a synthetic template (4.5 mm × 7.0 mm) was performed using ex situ AFM. The template samples were taken out of the solution, followed by washing with deionized water and drying with N_2 gas before visualization. No mica was needed for the AFM analysis of template samples. In the case of the AFM analysis of Aβ aggregates grown in a solution, 6 μL aliquots of an Aβ sample were deposited onto freshly cleaved mica and incubated for a few minutes at room temperature. Samples were subsequently rinsed twice with 50 μL of deionized water and dried with N_2. AFM images were acquired on a Nanoscope III multimode atomic force microscope using an "E"-type scanner (Digital Instruments Inc., California) under ambient conditions. Samples were imaged at a scan rate of 1−2 Hz in a tapping mode, and images were acquired at a resolution of 512 × 512 pixels. AFM tips with resonant frequency in the range 306−444 kHz were used. SPIP software (Image Metrology, Denmark) was used to measure and analyze the volume and height distributions of amyloid deposits on the template. At least two different samples and five spots among the entire areas were analyzed in each case. Representative images were selected for comparative studies.

ThT-Induced Fluorescence. Amyloid deposits that formed on the template were quantitatively characterized by ThT-induced fluorescence. Different concentrations of fresh Aβ on the synthetic template (8 mm × 18 mm) were incubated at 37 °C. The template samples were washed and dried before ThT fluorescence measurements. A 2 mL sample of ThT solution (50 μM) in Tris−HCl buffer (pH 8.0, 20 mM) was added to the 10 mm long path of a quartz cuvette. After the template samples were placed diagonally into a quartz cuvette containing a ThT solution, fluorescence measurements were carried out with a spectrofluorometer (model RF5301, Shimadzu Co., Japan). For each sample, the ThT intensity at 482 nm was obtained by subtracting the intensity of a control (0 μM Aβ) from the intensity of each sample.

FT-IR Spectroscopy. Attenuated total reflection (ATR) FT-IR spectra were obtained using a Nicolet Nexus 470 spectrometer (Thermo Nicolet Corp., Madison, WI) equipped with a single-bounce ATR accessory. Infrared spectra were acquired at a resolution of 4.0 cm^{-1} by placing and pressing solid samples on a rounded diamond crystal. To get absorbance spectra for different Aβ42 samples, the background spectrum of a plain glass was subtracted from the sample spectra.

Results

Amyloid Plaque-like Aggregate Growth on a Synthetic Template. According to the amyloid cascade hypothesis,[3,14] the deposition of Aβ42 diffuse plaques is an initial step that may be associated with AD pathogenesis. In this study, 12 h preincubated, fibril-free, Aβ42 oligomers were immobilized onto an NHS-activated solid surface to mimic the deposition of Aβ42 diffuse plaques in the early event of the amyloid cascade hypothesis. Aβ42 oligomers were produced by the incubation of fresh Aβ42 monomers prepared by a series of treatments with HFIP and DMSO. Previous studies demonstrated that HFIP-treated Aβ42 in DMSO provides a uniform, unaggregated Aβ42.[15,16] An AFM analysis of the 12 h incubated Aβ42 solution confirmed the

(13) Ha, C.; Park, C. B. *Biotechnol. Bioeng.* **2005**, *90*, 848−855.

(14) Hardy, J.; Selkoe, D. J. *Science* **2002**, *297*, 353−356.

(15) Stine, W. B.; Dahlgren, K. N.; Krafft, G. A.; LaDu, M. J. *J. Biol. Chem.* **2003**, *278*, 11612−11622.

(16) Chromy, B. A.; Nowak, R. J.; Lambert, M. P.; Viola, K. L.; Chang, L.; Velasco, P. T.; Jones, B. W.; Fernandez, S. J.; Lacor, P. N.; Horowitz, P.; Finch, C. E.; Krafft, G. A.; Klein, W. L. *Biochemistry* **2003**, *42*, 12749−12760.

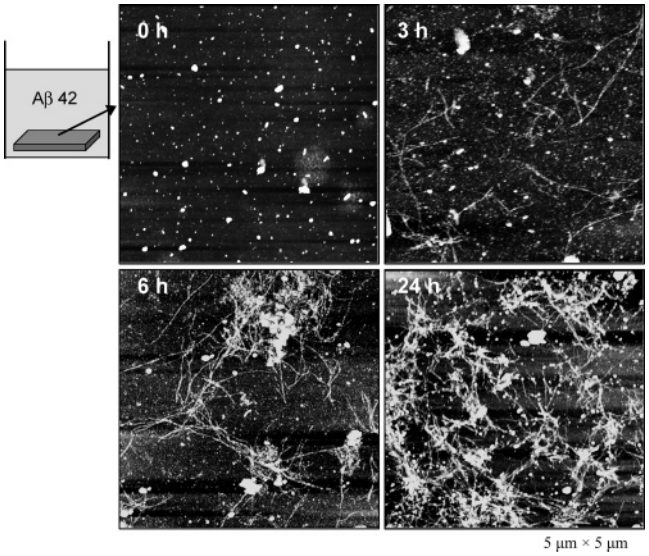

Figure 1. Representative AFM images of Aβ42 aggregates formed on a synthetic template. The template was prepared by immobilizing a 12 h preincubated Aβ42 solution (30 μM) on an NHS-activated solid surface. After the treatment, the template was incubated in a fresh Aβ42 (30 μM) at pH 7.4 and 37 °C for 0, 3, 6, and 24 h, followed by ex situ AFM analysis of the surface of each sample.

presence of Aβ42 oligomers with 4 ± 2 nm *z* height and the absence of rod-shaped protofibrils and fibrils (data not shown). According to Roher et al.,[17] *z* height values of Aβ aggregates in the range of 2−5 nm measured by AFM were estimated to correspond to oligomeric molecular masses ranging from 10 to 100 kDa.

To observe the growth of amyloid plaque-like aggregates on the synthetic template, we incubated the template immobilized with Aβ42 oligomers in a fresh Aβ42 solution (30 μM, pH 7.4) at 37 °C. The temporal evolution of amyloid growth was visually observed with ex situ AFM. An AFM image at 0 h (Figure 1, 0 h) shows the presence of initial Aβ42 oligomers as seeds that worked to support further amyloid growth. A higher magnification image and lateral size of 0 h Aβ42 oligomers as seeds were obtained using section analysis (Figure 2). This image was further reconstructed into 3-D shape, which shows a number of small spherical aggregates (Figure 3, 0 h). According to the height distribution analysis, the thickness of most Aβ42 oligomers was in the range of ∼7 nm (Figure 4, 0 h). After 3 h of incubation, a few fibrils and amorphous aggregates were observed (Figure 1, 3 h), which indicates that preexisting Aβ42 aggregates were effective seeds to induce the transition of soluble Aβ to insoluble amyloid aggregates on the template. After 6 h of incubation, amorphous aggregates and ordered amyloid aggregates in a fibrillar form appeared throughout the entire region (Figure 1, 6 h). Dense-cored amyloid aggregates, like the forest of twisted fibrils, were formed at 24 h of incubation (Figure 1, 24 h). The topological structure of the amyloid aggregates was visualized as a 3-D image in Figure 3 (24 h). Height distributions represented by Gaussian curves continuously shifted to the right, indicating the gradual deposition of Aβ42 onto the template (Figure 4). The mean height of the insoluble aggregates incubated for 24 h was ∼15 nm (Figure 4). For a quantitative analysis of the plaque-like aggregate growth, the total volume of amyloid aggregates formed on the template was assessed by multiplying and summating the height of numerous Aβ42 deposits by their frequency. As shown in the inset of Figure 4, the overall volume of deposited aggregates gradually increased from 0 to 24 h of incubation.

The aggregates grown on the synthetic template were further characterized with ThT-induced fluorescence and FT-IR. ThT had been known to associate rapidly with amyloid aggregates, giving rise to a new emission maximum at around 482 nm.[18] According to Figure 5a, ThT-induced fluorescence increased in a concentration-dependent manner with a stronger intensity of fluorescence at a higher Aβ42 concentration in a solution phase, which indicates that the transition of fresh Aβ42 into an amyloid form occurred on the template surface. The conformational change of Aβ42 deposits on the template over time was analyzed using FT-IR. The absorbance spectra in Figure 5b show predominant peaks at 1629 and 1542 cm^{-1}, which correspond to amide I and II bands, respectively. Previous studies indicated that the amide I and II bands are very sensitive to changes in the secondary structure of Aβ42 peptides.[19,20] A strong absorption peak at 1629 cm^{-1} was known to represent an antiparallel β-sheet structure. Thus, progressive increase of a peak at 1629 cm^{-1} in Figure 5b should be associated with continuous conversion of soluble Aβ42 to amyloid fibrils with antiparallel β-sheet structure on the template.

Using ex situ AFM, we analyzed the temporal evolution of Aβ42 in the "solution" phase where the synthetic amyloid template was incubated. As shown in Figure 6a, amyloid aggregates such as protofibrils and fibers were observed in the solution after 24 h of incubation. Interestingly, the morphology of amyloid aggregates in the solution phase was significantly different from those on the template. While relatively thin fibrillar plaques with faintly discernible crossover repeats formed on the template surface, the distinct ropelike shape of short and thick protofibrils and fibrils was observed in the solution (Figure 6a, 24 h, inset). Such morphological differences might result from the different degrees of lateral association between protofilaments or fibers in a solution and on a solid surface. Template-directed grown fibrils should lack a lateral association of protofilaments or fibers because of their tight binding to the template surface. The gradual decrease of total Aβ amounts in the solution phase in the presence of the template was observed according to the time profile of height analysis (Figure 7), which should be caused by the deposition of soluble Aβ peptides onto the template surface. In contrast to the template surface (Figure 4), the heights of Aβ aggregates in the solution in the presence of the template decreased from a range of 4−8 nm to one of ∼2 nm over an incubation time of 24 h (Figure 7). As a control experiment, 12 h preincubated Aβ42 oligomers were added to a fresh Aβ42 solution. This solution was incubated in the "absence" of the template. In this case, no amyloid aggregates or fibrils were found in solution, even after 24 h of incubation (Figure 6b) or longer. According to AFM analysis, mostly unaggregated Aβ and a few large Aβ aggregates were present at the initial incubation time (Figure 6b, 0 h), while the size of Aβ aggregates became more homogeneous after 6 h (Figure 6b, 6 h).

Effects of Fresh, Oligomeric, and Fibrillar Aβ Seeds on Amyloid Aggregate Growth. Earlier works suggested that diffuse plaques were pre-amyloid deposits that may trigger amyloid formation in vivo,[1,3] but the seeding capability of diffuse plaques for amyloid growth had rarely been studied. To investigate the effects of diffuse plaques on amyloid plaque growth, three different kinds of Aβ seeds were prepared: fresh monomers, oligomers, and fully grown fibrils. Relative seeding efficiencies

(17) Roher, A. E.; Baudry, J.; Chaney, M. O.; Kuo, Y.-M.; Stine, W. B.; Emmerling, M. R. *Biochim. Biophys. Acta* **2000**, *1502*, 31−43.
(18) LeVine, H., III. *Protein Sci.* **1993**, *2*, 404−410.
(19) Lin, S.-Y.; Chu, H.-L. *Int. J. Biol. Macromol.* **2003**, *32*, 173−177.
(20) Lashuel, H. A.; LaBrenz, S. R.; Woo, L.; Serpell, L. C.; Kelly, J. W. *J. Am. Chem. Soc.* **2000**, *122*, 5262−5277.

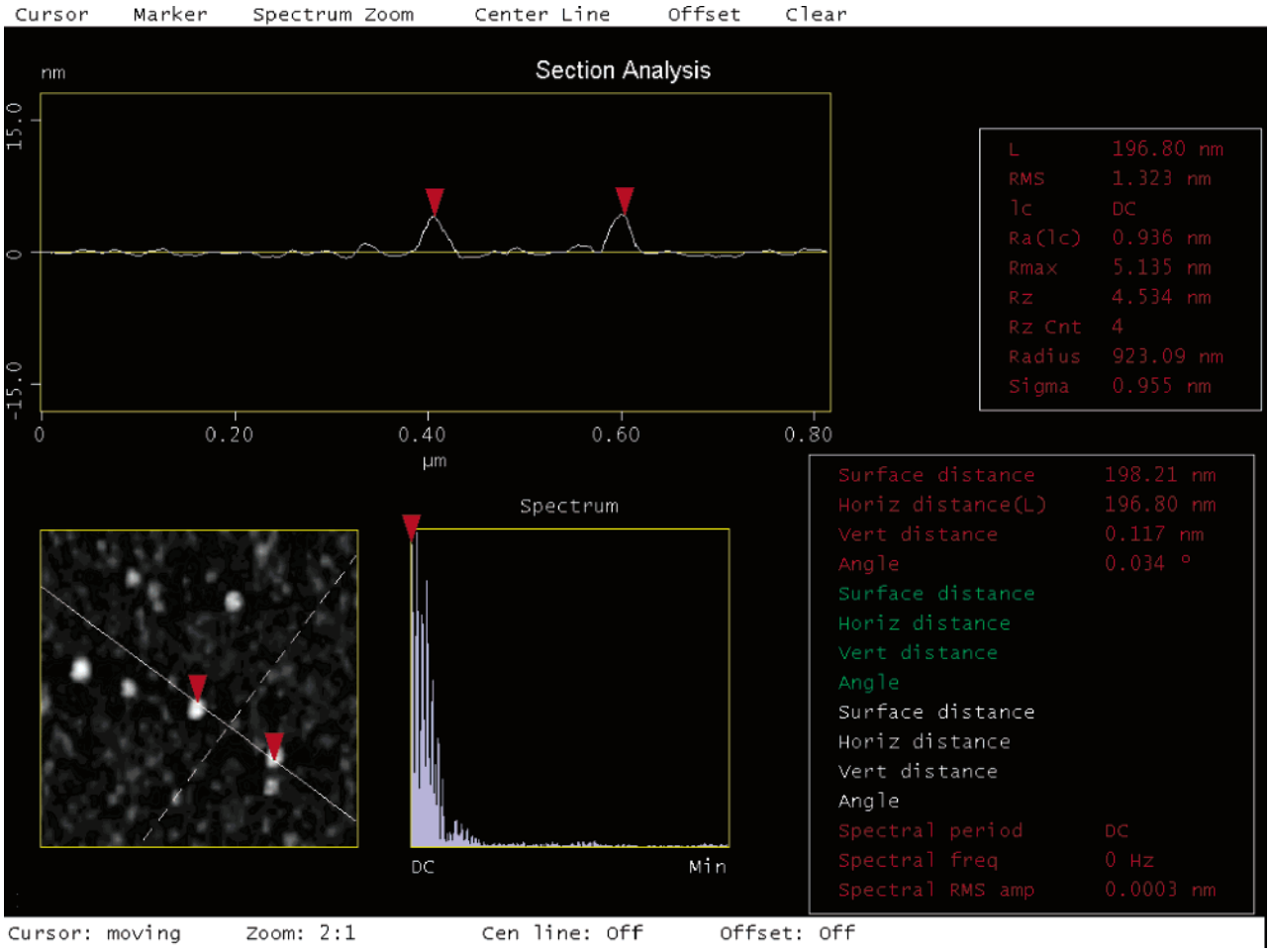

Figure 2. Higher magnification images and section analysis of 0 h Aβ42 oligomers as seeds.

were investigated by measuring the height distribution and aggregate volume change on the synthetic template. Figure 8 shows that 12 h preincubated Aβ oligomers were more efficient than fully grown Aβ fibrils for further plaque growth. Moreover, fresh Aβ peptides were found to be good seeds to induce amyloid fibrils, according to the aggregate volume change (Figure 8, inset) and height distribution analysis (Figure 8). As a control experiment, a template immobilized with bovine serum albumin rather than Aβ was incubated with a fresh solution of Aβ42 (30 μM, pH 7.4) at 37 °C. According to AFM analysis, very small amounts of amyloid deposits were observed after 24 h of incubation (Figure 9). These observations suggest that Aβ deposition on the surface is a critical step leading to the growth of amyloid plaques and that the deposition of early products in the amyloid fibrillogenesis pathway, such as Aβ monomers and oligomers, can act as efficient seeds to promote further amyloid plaque formation in vivo. These results also support the previous report by Koppaka et al.[21] that the binding of Aβ to a plasma membrane may be an important step in amyloid plaque formation.

Interaction between Aβ40 and Aβ42 during Amyloid Aggregate Growth. The presence of both Aβ40 and Aβ42 in neuritic plaques[3] prompted us to study which species plays a more important role in amyloid formation and growth. Here, the interactive roles of Aβ42 and Aβ40 in amyloid formation and growth were analyzed according to the height distribution and volume change of amyloid aggregates grown under three combinations of the peptides: (1) Aβ40 on a template/Aβ40 in solution, (2) Aβ40 on a template/Aβ42 in solution, (3) Aβ42 on a template/Aβ40 in solution, and (4) Aβ42 on a template/Aβ42 in solution. It was found that the plaque growth was maximized by Aβ42 deposition on Aβ42 seeds (Figure 10). The volume of aggregates observed by Aβ40 deposition on Aβ40 seeds (Figure 10b, inset) was the lowest, showing the lowest number of tangled fibrils (Figure 10a). These comparative experiments indicate that Aβ42 may contribute to amyloid plaque growth more than Aβ40. This result supports a previous report[3] that Aβ42 constitutes a larger portion of total Aβ peptides in amyloid plaques, although Aβ40 is the most predominant soluble species in the blood and cerebrospinal fluid. It is noteworthy that the change of seeds from Aβ42 to Aβ40 decreased the extent of amyloid plaque formation on Aβ42 seeds (Figure 10b).

Effects of Solution pH on the Morphology of Aβ Aggregates. The change of solution pH had been known to be one of the important environmental factors that affect the conformational change of Aβ peptides,[22] but little was known about the effect of pH on amyloid deposition and growth. According to our study, solution pH significantly influences the morphology of amyloid aggregates grown on a template surface. As shown in Figure 11, the AFM analysis indicates that amyloid aggregates became dominant in the "fibrillar" form at pH 7.4 and 6.9. On the contrary, "amorphous" aggregates were predominantly found on the template when incubated in the solution at pH 6.4−4.9. The

(21) Koppaka, V.; Paul, C.; Murray, I. V. J.; Axelsen, P. H. *J. Biol. Chem.* **2003**, *278*, 36277−36284.

(22) Matsunaga, Y.; Îerovnik, E.; Yamada, T.; Turk, V. *Curr. Med. Chem.* **2002**, *9*, 1717−1724.

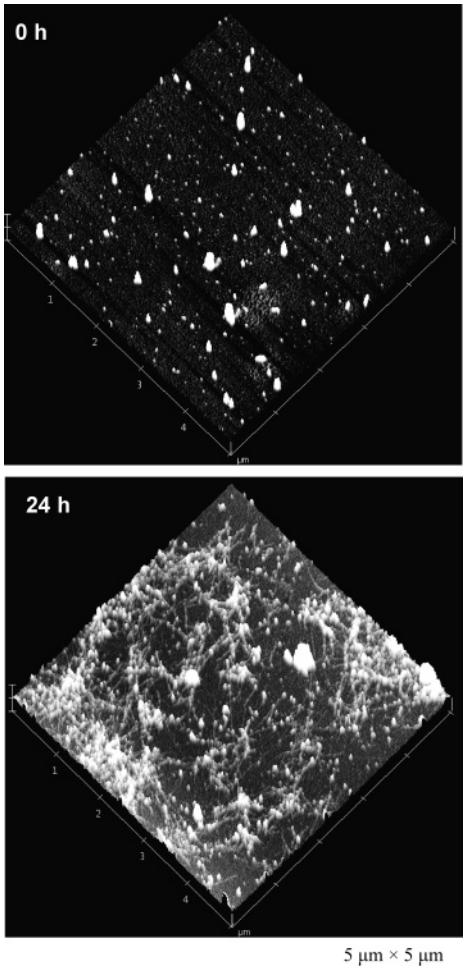

Figure 3. 3-D AFM images of Aβ42 plaque-like aggregates formed on a template. The same samples used for Figure 1 (0, 24 h) were observed here in 3-D mode for the visualization of topological details of Aβ42 aggregates formed on the template.

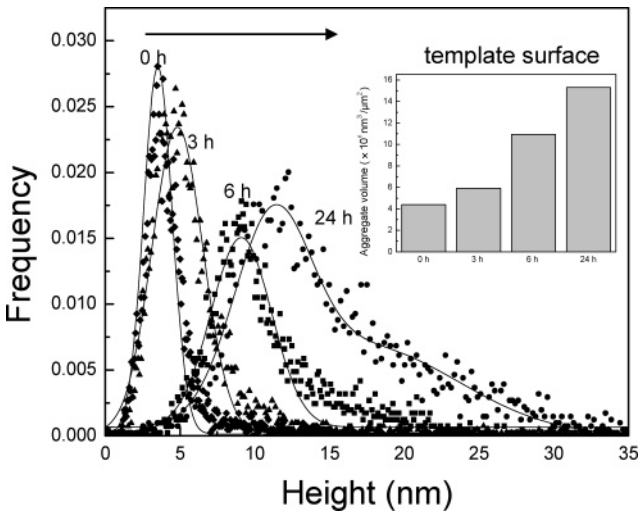

Figure 4. Height distribution change of the Aβ42 deposition with time on the solid template. AFM images shown in Figure 1 were quantitatively analyzed using SPIP software. Data were fitted with Gaussian curves. Inset: time evolution of the total aggregate volume on the template. The amyloid aggregate volume on a template was evaluated by multiplying the height of each Aβ42 deposit by its frequency followed by the summation of all the values.

reappearance of several amyloid fibrils at pH 4.9 indicates that acidic pH lower than 5.0 may also induce amyloid fibril formation. A previous study showed that acidic pH accelerates the formation of amyloid fibrils.[15] According to histogram analysis, the total amount of aggregates formed on the template was much higher at pH 7.4 compared to lower pHs (data not shown). This result with a synthetic template is in accordance with a previous report showing that the deposition rates of soluble Aβ on preexisting amyloid plaques in human brain tissue were maximized at around neutral pH with a decreasing deposition rate at a slightly lower pH.[23] These observations suggest that a slightly lower pH may not be a favorable condition for amyloid growth.

Discussion

Amyloid deposition, the process of amyloid plaque growth by the conversion of soluble Aβ peptides in a solution phase to insoluble amyloid fibrils on a solid surface, is one of the key pathological features of AD. To understand the underlying etiology of AD, it is important to elucidate the effects of environmental factors that influence the amyloid deposition process. According to the amyloid cascade hypothesis,[1,3,14] diffuse plaques are initial and visual deposits in the early event of AD, and they are observed as metastable intermediates during the process of amyloid plaque growth on brain tissue. In the current work, different types of synthetic templates were prepared by immobilizing three kinds of Aβ aggregates (i.e., fresh Aβ42, 12 h preincubated Aβ42 oligomers, and fully grown amyloid fibrils) on an NHS-activated solid surface. According to both the height distribution and total volume change of amyloid aggregates on the template (Figure 8), 12 h preincubated Aβ42 oligomers were found to be the most efficient seeds to accelerate amyloid growth. On the basis of this observation, we suggest that amyloid plaque growth in vivo can be accelerated by the deposition of oligomeric Aβ42 aggregates in tissues or membranes rather than fresh or fibrillar forms of Aβ42. In support of this hypothesis, earlier works[24,25] confirmed the presence of soluble Aβ oligomers in the cerebrospinal fluid of AD and the increase of their concentration prior to the appearance of fibrillar Aβ plaques. Synapse failure before neuron death in early AD had been considered to be caused by the accumulation of Aβ oligomers rather than amyloid fibrils.[26−28] Furthermore, oligomeric assemblies were a major component among fractions purified from neuritic cores and sheets of vascular amyloid by size exclusion chromatography.[29] Taken together, the results shown here indicate that the generation of Aβ42 oligomers and their deposition might be an important early step to induce further growth of neuritic plaques.

The template surface had a certain degree of heterogeneity with a Gaussian-type distribution of amyloid aggregates on the surface as indicated by the AFM section analysis (Figures 2 and 4). Despite the heterogeneity of the surface, the distribution pattern of the aggregates did not change significantly to affect the average thickness of the aggregates when we observed multiple spots on

(23) Esler, W. P.; Stimson, E. R.; Ghilardi, J. R.; Felix, A. M.; Lu, Y.-A.; Vinters, H. V.; Mantyh, P. W.; Maggio, J. E. *Nat. Biotechnol.* **1997**, *15*, 258−263.
(24) Pitschke, M.; Prior, R.; Haupt, M.; Riesner, D. *Nat. Med.* **1998**, *4*, 832−834.
(25) Teller, J. K.; Russo, C.; Debusk, L. M.; Angelini, G.; Zaccheo, D.; Dagna-Bricarelli, F.; Scartezzini, P.; Bertolini, S.; Mann, D. M. A.; Tabaton, M.; Gambetti, P. *Nat. Med.* **1996**, *2*, 93−95.
(26) Lacor, P. N.; Buniel, M. C.; Chang, L.; Fernandez, S. J.; Gong, Y.; Viola, K. L.; Lambert, M. P.; Velasco, P. T.; Bigio, E. H.; Finch, C. E.; Krafft, G. A.; Klein, W. L. *J. Neurosci.* **2004**, *24*, 10191−10200.
(27) Kayed, R.; Head, E.; Thompson, J. L.; Mclntire, T. M.; Milton, S. C.; Cotman, C. W.; Glabe, C. G. *Science* **2003**, *300*, 486-489.
(28) Walsh, D. M.; Klyubin, I.; Fadeeva, J. V.; Rowan, M. J.; Selkoe, D. J. *Biochem. Soc. Trans.* **2002**, *30*, 552−557.
(29) Roher, A. E.; Chaney, M. O.; Kuo, Y.-M.; Webster, S. D.; Stine, W. B.; Haverkamp, L. J.; Woods, A. S.; Cotter, R. J.; Tuohy, J. M.; Krafft, G. A.; Bonnell, B. S.; Emmerling, M. R. *J. Biol. Chem.* **1996**, *271*, 20631−20635.

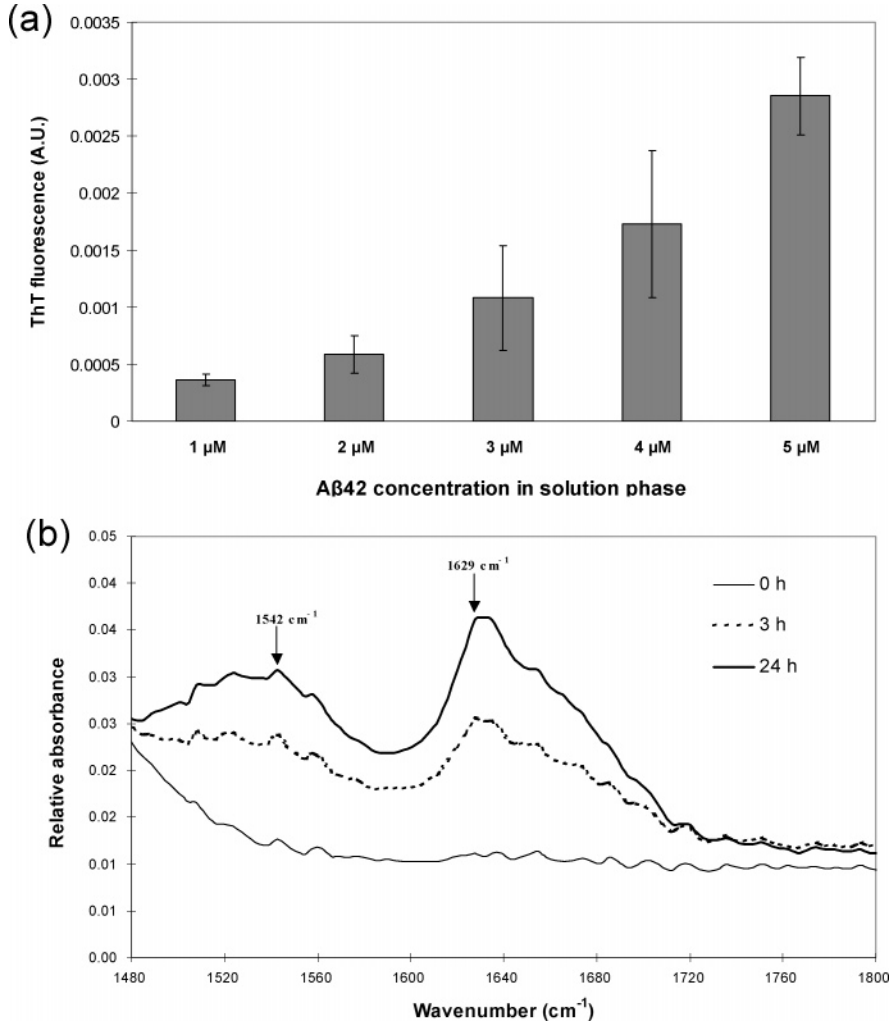

Figure 5. ThT-induced fluorescence and FT-IR spectra of Aβ42 aggregates formed on the template. (a) Concentration dependency of Aβ42 plaque growth on the template according to ThT-induced fluorescence analysis. An amyloid template was incubated in solutions having different Aβ42 concentrations (1−5 μM) for 6 h at pH 7.4 and 37 °C. The amyloid aggregates grown on each template after 6 h were measured in triplicate using ThT-induced fluorescence. (b) Time-dependent changes in FT-IR spectra of Aβ42 aggregates formed on the template. Samples were prepared by incubating the template in Aβ42 solution (30 μM) at pH 7.4 and 37 °C for 0, 3, and 24 h.

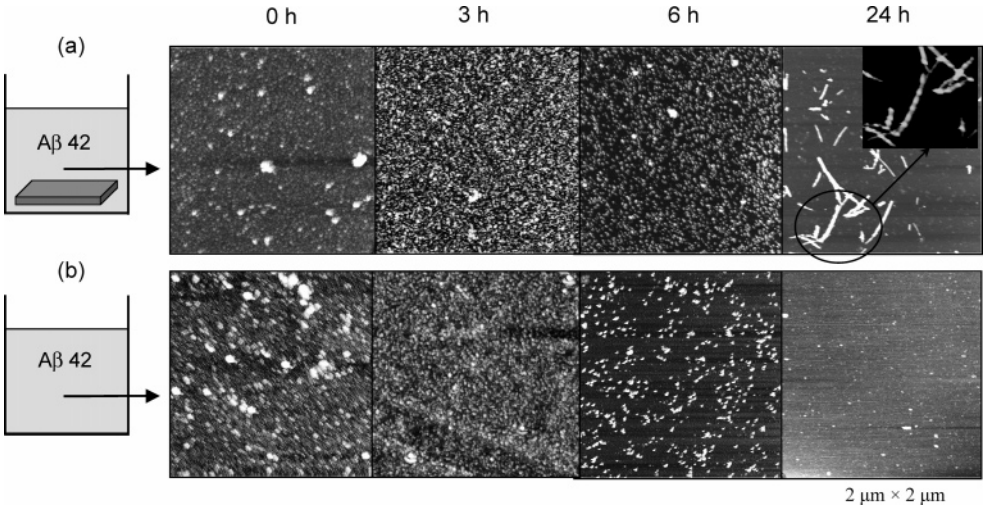

Figure 6. Representative AFM images of (a) Aβ42 aggregation in the solution phase in the presence of the template and (b) Aβ42 aggregation in a template-free solution where 12 h preincubated Aβ42 oligomers as seeds were added. A 30 μM concentration of Aβ42 was initially present in each solution at pH 7.4 and 37 °C, and the solution was incubated for 24 h with or without a synthetic template. The template was prepared by immobilizing a 12 h preincubated Aβ42 solution (30 μM) on an NHS-activated solid surface.

the same template surface at each time (data not shown). This observation implies that the surface heterogeneity may not influence significantly the seeding process and the subsequent amyloid deposition and growth. The representative AFM images

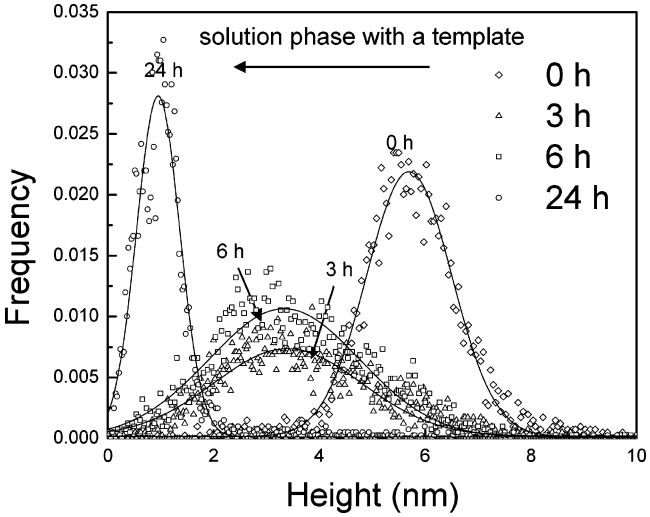

Figure 7. Height distribution change of the Aβ42 aggregates with time in the solution phase in the presence of the template. AFM images in Figure 5a were quantitatively analyzed using SPIP software. Data were fitted with Gaussian curves. The arrow indicates the gradual decrease of total Aβ aggregate amounts in the solution phase in the presence of the template.

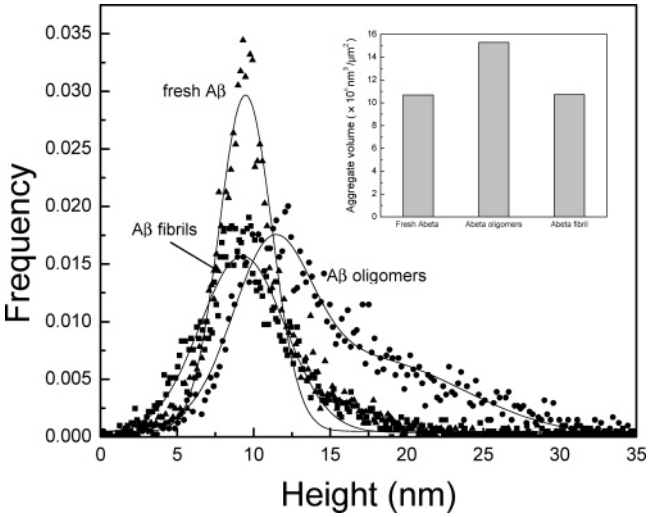

Figure 8. Effects of seed condition on amyloid growth. Each template was in Aβ42 solution (30 μM) with different seeds on the surface, such as fresh Aβ42, 12 h preincubated Aβ42 oligomers, and fully grown fibers for 24 h. In each case, the same volume of aliquots (7 μL) was withdrawn and immobilized to an NHS-activated solid surface. The inset compares the total volumes of aggregates grown on the template with different types of seeds.

were selected for comparative studies in this paper. According to our height distribution analysis, the average thickness of Aβ42 oligomers or seeds was in the range of ∼7 nm, which grew to have a mean height of ∼15 nm after 24 h of incubation (Figure 4).

The balance between Aβ production and clearance in the cerebrospinal fluid phase was known to be one of the important factors in the amyloid cascade flow.[14] Our result shows that the formation of insoluble amyloid aggregates can serve as a sink of soluble Aβ in the solution phase by attracting them onto the solid surface as well as to accelerate the formation of intermediates in the pathway of amyloid fibrillation in a solution. This speculation is supported by previous reports showing that the metabolism and clearance of soluble Aβ can be caused by the formation of insoluble amyloid plaques in the brain tissue.[30] According to previous studies, the amount of insoluble plaques

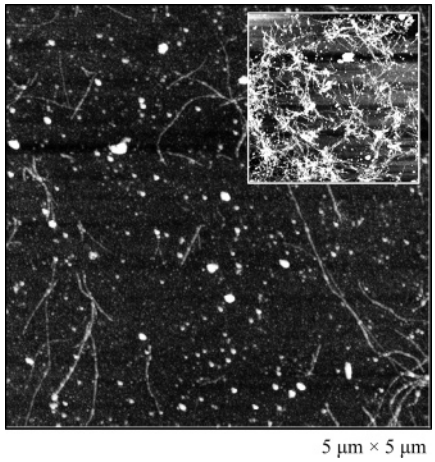

Figure 9. An AFM image of Aβ42 aggregates formed on the template surface immobilized with 1% BSA (instead of Aβ42). An NHS-activated template was treated with BSA solution (1%, w/v), followed by incubation in Aβ42 solution (30 μM) for 24 h. The AFM image of Aβ42 aggregates grown on an Aβ42 template for 24 h (Figure 1, 24 h) is included as an inset for comparison.

increases during plaque deposition, but the amount of soluble Aβ in the brain does not increase to the same extent.[31,32] It is noteworthy that amyloid plaques in AD and Lewy bodies in Parkinson's disease had been considered reservoirs of potentially toxic proteins in the brain.[14] The complexity of equilibrium between different Aβ species and the difficulties in measuring an exact concentration of each species, however, may pose as obstacles to unveiling the mechanism of amyloid plaque formation in vivo.

The analysis of the interactive role between Aβ40 and Aβ42 in amyloid formation may help explain their different contributions in amyloid plaque growth in vivo. An earlier study showed that mixed species of Aβ40 and Aβ42 are generally found in neuritic plaques, although diffuse plaques consist mostly of Aβ42.[3] Our result, based on AFM images and height distribution analysis (Figure 10), reveals that amyloid growth is most accelerated by "Aβ42 on a template/Aβ42 in solution" rather than other cases. A previous report noted that the increase of the Aβ42:Aβ40 ratio was closely related to familiar forms of early onset AD.[33] Moreover, it was demonstrated that presenilin mutations selectively produce increased amounts of Aβ42 deposition in AD patients.[34,35] Also, Aβ42 is known to be a predominant species in neuritic plaques even though the concentration of secreted Aβ42 is only about 10% of the Aβ40 concentration.[36] The difference between Aβ42 and Aβ42 in amyloid deposition or aggregation may come from additional hydrophobic Ile−Ala residues located in the C-terminal part of Aβ42.[9] Hydrophobic interactions had been known to be one of the major driving forces for Aβ oligomerization and fibril formation.[15]

(30) DeMattos, R. B.; Bales, K. R.; Cummins, D. J.; Paul, S. M.; Holtzman, D. M. *Science* **2002**, *295*, 2264−2267.
(31) Wang, J.; Dickson, D. W.; Trojanowski, J. Q.; Lee, V. M. Y. *Exp. Neurol.* **1999**, *158*, 328−337.
(32) Naslund, J.; Haroutunian, V.; Mohs, R.; Davis, K. L.; Davies, P.; Greengard, P.; Buxbaum, J. D. *JAMA, J. Am. Med. Assoc.* **2000**, *283*, 1571−1577.
(33) Scheuner, D.; Eckman, C.; Jensen, M.; Song, X.; Citron, M.; Suzuki, N.; Bird, T. D.; Hardy, J.; Hutton, M.; Kukull, W.; Larson, E.; Levy-Lahad, L.; Viitanen, M.; Peskind, E.; Poorkaj, P.; Schellenberg, G.; Tanzi, R.; Wasco, W.; Lannfelt, L.; Selkoe, D.; Younkin, S. *Nat. Med.* **1996**, *2*, 864−870.
(34) Lemere, C. A.; Lopera, F.; Kosik, K. S.; Lendon, C. L.; Ossa, J.; Saido, T. C.; et al. *Nat. Med.* **1996**, *2*, 1146−1150.
(35) Mann, D. M.; Iwatsubo, T.; Cairns, N. J.; Lantos, P. L.; Nochlin, D.; Sumi, S. M.; et al. *Ann. Neurol.* **1996**, *40*, 149−156.
(36) Gravina, S. A.; Ho, L.; Eckman, C. B.; Long, K. E.; Otvos, L.; Younkin, L. H.; Suzuki, N.; Younkin, S. G. *J. Biol. Chem.* **1995**, *270*, 7013−7016.

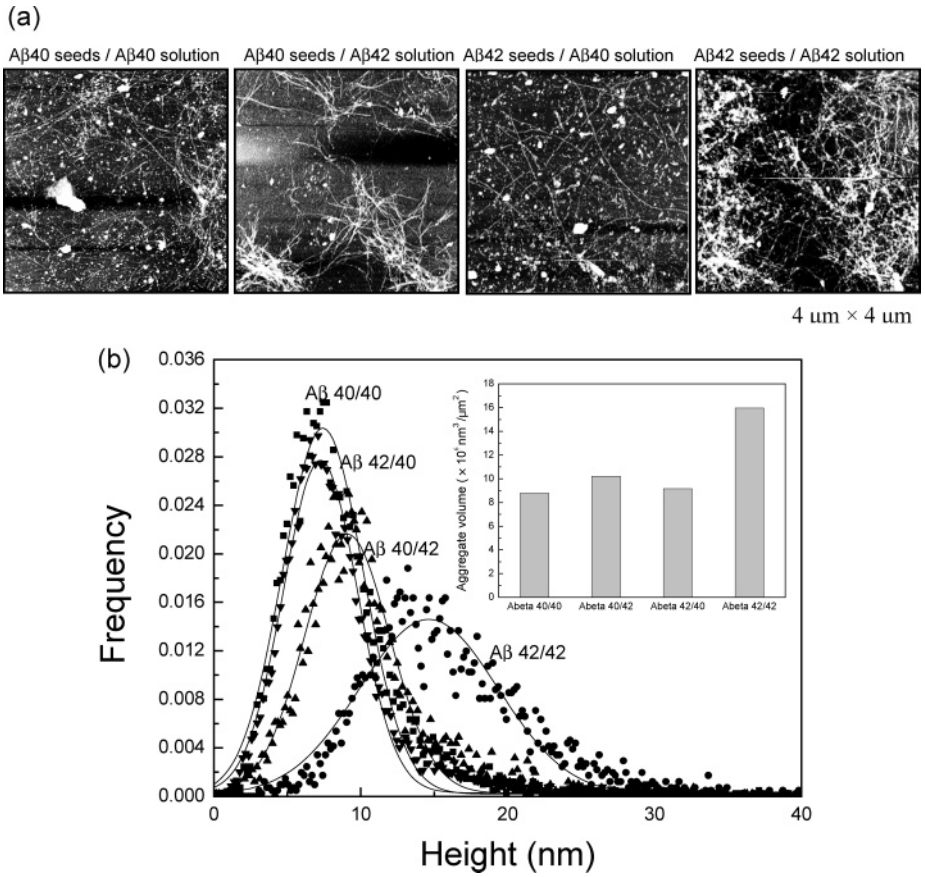

Figure 10. Interaction between Aβ40 and Aβ42 during the amyloid growth on a template: (a) representative AFM images and (b) height distribution of AFM images and aggregate volume changes in the inset. A synthetic template with 12 h preincubated Aβ40 or Aβ42 seeds was incubated in Aβ40 or Aβ42 solution (30 μM) for 24 h at pH 7.4 and 37 °C.

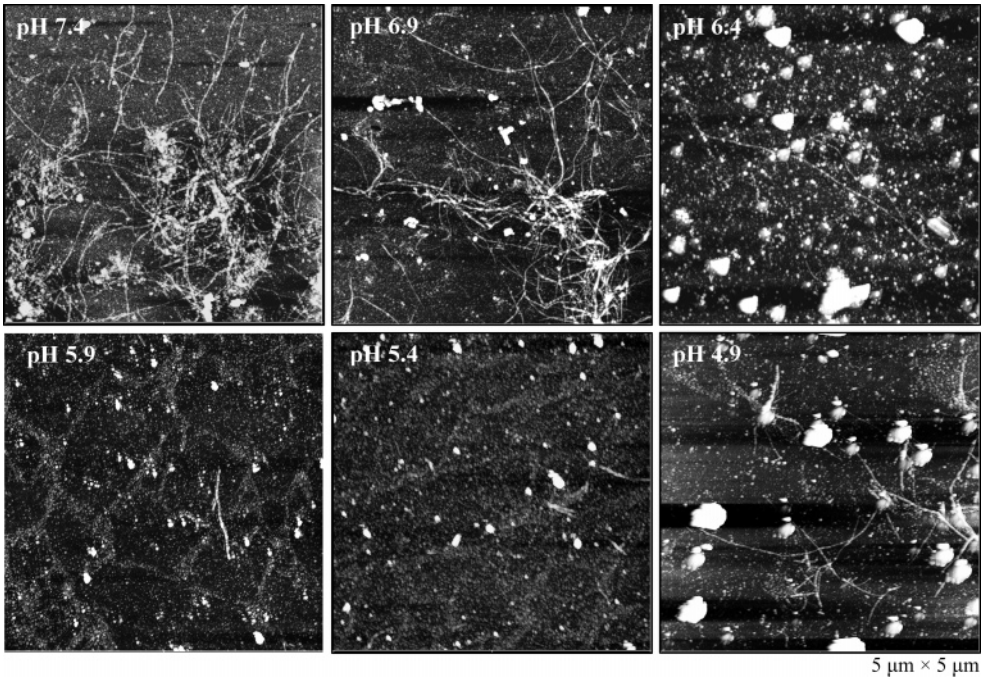

Figure 11. Effect of solution pH on Aβ42 deposition and aggregate formation on the template. For AFM analysis, each synthetic template was incubated in Aβ42 solution (30 μM) at pH 7.4, 6.9, 6.4, 5.9, 5.4, and 4.9 for 6 h at 37 °C.

The generation of Aβ by means of the proteolytic processing of APP had been known to take place in a slightly lower pH compartment of the cell, though it is not yet clearly known whether plaque formation or amyloid deposition occurs at a low pH in vivo.[37] Our results indicate that the slightly lower pH may lead to the formation of amorphous aggregates rather than fibrillar

(37) Selkoe, D. J. *Annu. Rev. Neurosci.* **1994**, *17*, 489−517.

aggregates. The pH dependence of Aβ conformational changes may occur by means of protonation of amino acid residues and changes in their specific interaction.[38,39] In the pH range of 6.4−5.4, the imidazole ring of His may play an important role in the morphological changes of Aβ aggregates. Since the pK_a value of His is 6.0, the imidazole ring of His is likely to become protonated under pH lower than 6.0. Also, the conformational change may be dependent on the disruption of salt bridges between His13 and Asp23 or Asp23 and Lys28, which was known to be important to stabilize amyloid fibrils and β-sheet structures.[39,40] In support of the reports, the current work suggests that the changes of protonation and electrostatic interactions of Aβ at mildly low pHs might be responsible for amorphous aggregate formation.

In this study, we developed a synthetic template to mimic β-amyloid aggregate formation and deposition that occurs on human brain tissues at the early stages of AD. Our synthetic template was made by immobilization of Aβ42 oligomers on a functionalized glass. The results obtained with the synthetic template were consistent with those of previous studies using human brain tissues in terms of pH effect and concentration dependency of β-amyloid deposition.[23] Further improvement of the template, for example, the use of a cell lipid bilayer membrane, may need to be done in the near future to imitate in vivo amyloid plaque formation more closely. Such a study should help provide a significant forward step in the understanding of these slow, insidious, and intractable diseases.

Conclusions

The visualization of Aβ deposition and growth is important for the evaluation of AD and for testing the efficacy of therapeutic interventions.[43,44] The current study demonstrates the temporal evolution of Alzheimer's amyloid aggregates in vitro arising from oligomeric Aβ seeds on a solid template surface. It was shown that amyloid aggregates work as a sink of the soluble Aβ peptide and reservoirs of small aggregates such as oligomers and protofibrils. It was found that amyloid growth on the template was affected by environmental factors such as the types of Aβ seeds, the interaction between Aβ42 and Aβ40, and the solution pH. The synthetic template developed in this work may be a useful tool for studying amyloid deposition and growth in vitro.

LA0601511

(38) Fraser, P. E.; McLachlan, D. R.; Surewicz, W. K.; Mizzen, C. A.; Snow, A. D.; Nguyen, J. T.; Kirschner, D. A. *J. Mol. Biol.* **1994**, *244*, 64−73.
(39) Kirkitadze, M. D.; Condron, M. M.; Teplow, D. B. *J. Mol. Biol.* **2001**, *312*, 1103−1119.
(40) Ma, B.; Nussinov, R. *Proc. Natl. Acad. Sci. U.S.A.* **2002**, *99*, 14126−14131.
(41) Verdier, Y.; Zarandi, M.; Penke, B. *J. Pept. Sci.* **2004**, *10*, 229−248.
(42) Esler, W. P.; Stimson, E. R.; Jennings, J. M.; Vinters, H. V.; Ghilardi, J. R.; Lee, J. P.; Mantyh, P. W.; Maggio, J. E. *Biochemistry* **2000**, *39*, 6288−6295.
(43) Lee, S.-P.; Falangola, M. F.; Nixon, R. A.; Duff, K.; Helpern, J. A. *Magn. Reson. Med.* **2004**, *52*, 538−544.
(44) Hanzel, D. K.; Trojanowski, J. Q.; Johnston, R. F.; Loring, J. F. *Nat. Biotechnol.* **1999**, *17*, 53−57.